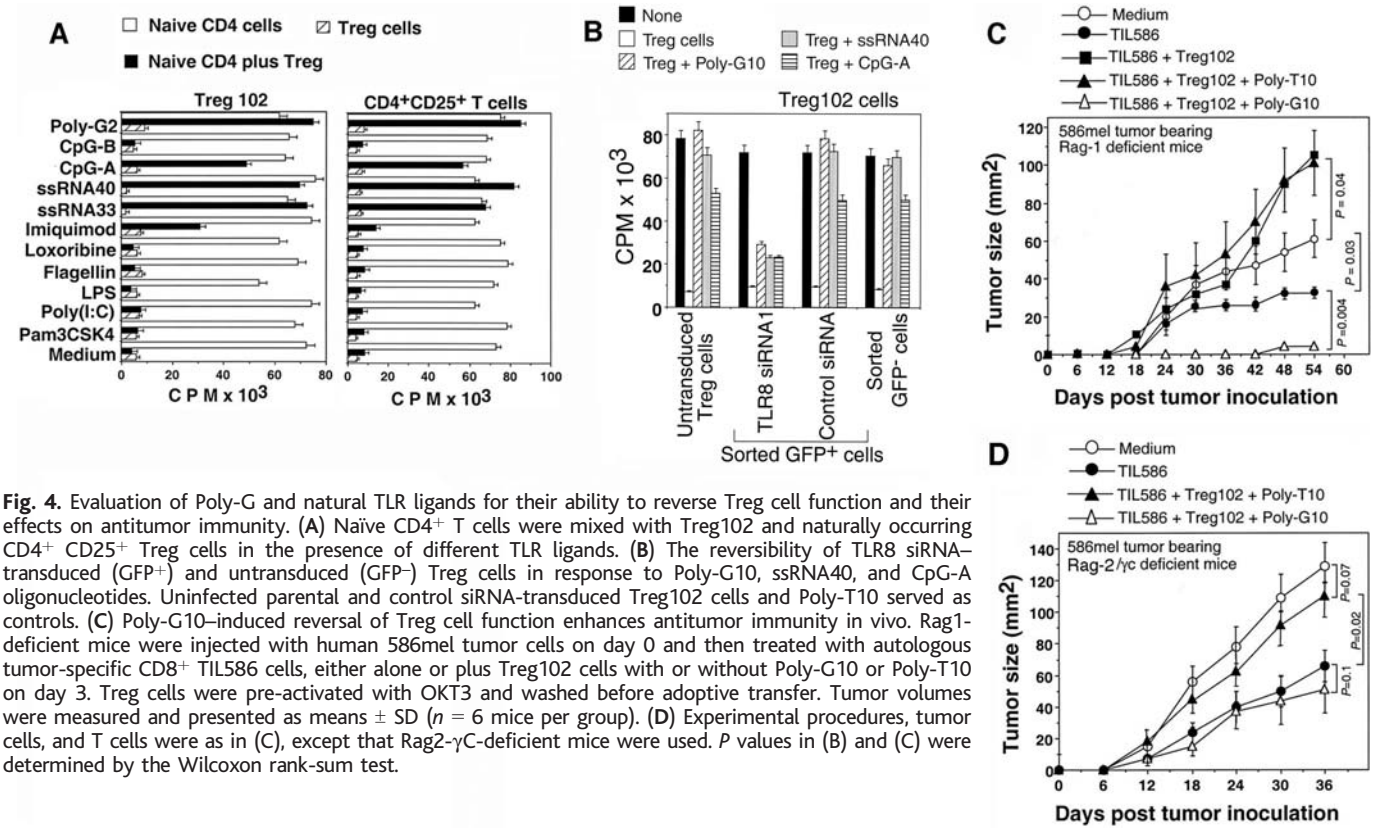

Fig. 4. Evaluation of Poly-G and natural TLR ligands for their ability to reverse Treg cell function and their effects on antitumor immunity. (**A**) Naïve $CD4^+$ T cells were mixed with Treg102 and naturally occurring $CD4^+$ $CD25^+$ Treg cells in the presence of different TLR ligands. (**B**) The reversibility of TLR8 siRNA–transduced (GFP^+) and untransduced (GFP^-) Treg cells in response to Poly-G10, ssRNA40, and CpG-A oligonucleotides. Uninfected parental and control siRNA-transduced Treg102 cells and Poly-T10 served as controls. (**C**) Poly-G10–induced reversal of Treg cell function enhances antitumor immunity in vivo. Rag1-deficient mice were injected with human 586mel tumor cells on day 0 and then treated with autologous tumor-specific $CD8^+$ TIL586 cells, either alone or plus Treg102 cells with or without Poly-G10 or Poly-T10 on day 3. Treg cells were pre-activated with OKT3 and washed before adoptive transfer. Tumor volumes were measured and presented as means ± SD (n = 6 mice per group). (**D**) Experimental procedures, tumor cells, and T cells were as in (C), except that Rag2-γC-deficient mice were used. P values in (B) and (C) were determined by the Wilcoxon rank-sum test.

25. J. M. Lund *et al.*, *Proc. Natl. Acad. Sci. U.S.A.* **101**, 5598 (2004).
26. R.-F. Wang, P. F. Robbins, Y. Kawakami, X. Q. Kang, S. A. Rosenberg, *J. Exp. Med.* **181**, 799 (1995).
27. We thank D. Golenbock for the gift of MyD88 and TLR9 cDNAs, L. Old and E. M. Shevach for discussion, M. Cubbage and C. Threeton for their assistance in FACS sorting, J. Gilbert for his assistance in the preparation of this manuscript, and anonymous reviewers for useful comments on the manuscript. Supported by grants from NIH (nos. R01CA90327, R01CA101795, P50CA58204, P50 CA093459, and PO1CA94237) and from the Cancer Research Institute.

Supporting Online Material
www.sciencemag.org/cgi/content/full/309/5739/1380/DC1
Materials and Methods
Figs. S1 to S6
References and Notes

11 April 2005; accepted 28 July 2005
10.1126/science.1113401

Molecular Mechanism for Switching of *P. falciparum* Invasion Pathways into Human Erythrocytes

Janine Stubbs,[1,2] Ken M. Simpson,[1] Tony Triglia,[1] David Plouffe,[4] Christopher J. Tonkin,[1] Manoj T. Duraisingh,[1] Alexander G. Maier,[1] Elizabeth A. Winzeler,[3,4] Alan F. Cowman[1]*

The malaria parasite, *Plasmodium falciparum*, exploits multiple ligand-receptor interactions, called invasion pathways, to invade the host erythrocyte. Strains of *P. falciparum* vary in their dependency on sialated red cell receptors for invasion. We show that switching from sialic acid–dependent to –independent invasion is reversible and depends on parasite ligand use. Expression of *P. falciparum* reticulocyte–binding like homolog 4 (PfRh4) correlates with sialic acid–independent invasion, and PfRh4 is essential for switching invasion pathways. Differential activation of PfRh4 represents a previously unknown mechanism to switch invasion pathways and provides *P. falciparum* with exquisite adaptability in the face of erythrocyte receptor polymorphisms and host immune responses.

Plasmodium falciparum causes the most lethal form of malaria, a devastating disease responsible for vast morbidity and loss of life. Invasion of erythrocytes by malaria parasites involves complex interactions between multiple ligands and receptors (*1*). Some *P. falciparum* strains predominantly use ligands that bind to sialic acid–containing erythrocyte receptors, and invasion is compromised when red cells are treated with neuraminidase (*2*, *3*). In contrast, other strains use ligands that bind to receptors independently of sialic acid. W2mef parasites have the capacity to switch from sialic acid–dependent to –independent invasion by selection on neuraminidase-treated erythrocytes (*4*–*6*). Consequently, disruption of sialic acid–dependent ligand EBA175 in the strain W2mef (W2mefΔ175) was possible and also resulted in a switch from sialic acid–dependent to –independent invasion (*5*, *6*). The molecular basis of switching to sialic acid–independent invasion has been unknown.

[1]The Walter and Eliza Hall Institute of Medical Research, Melbourne, Victoria 3050, Australia. [2]Cooperative Research Centre for Vaccine Technology and Department of Medical Biology, The University of Melbourne, Victoria 3010, Australia. [3]The Scripps Institute, La Jolla, CA 92037, USA. [4]The Genomics Institute of the Novartis Research Foundation, San Diego, CA 92121, USA.

*To whom correspondence should be addressed. E-mail: cowman@wehi.edu.au

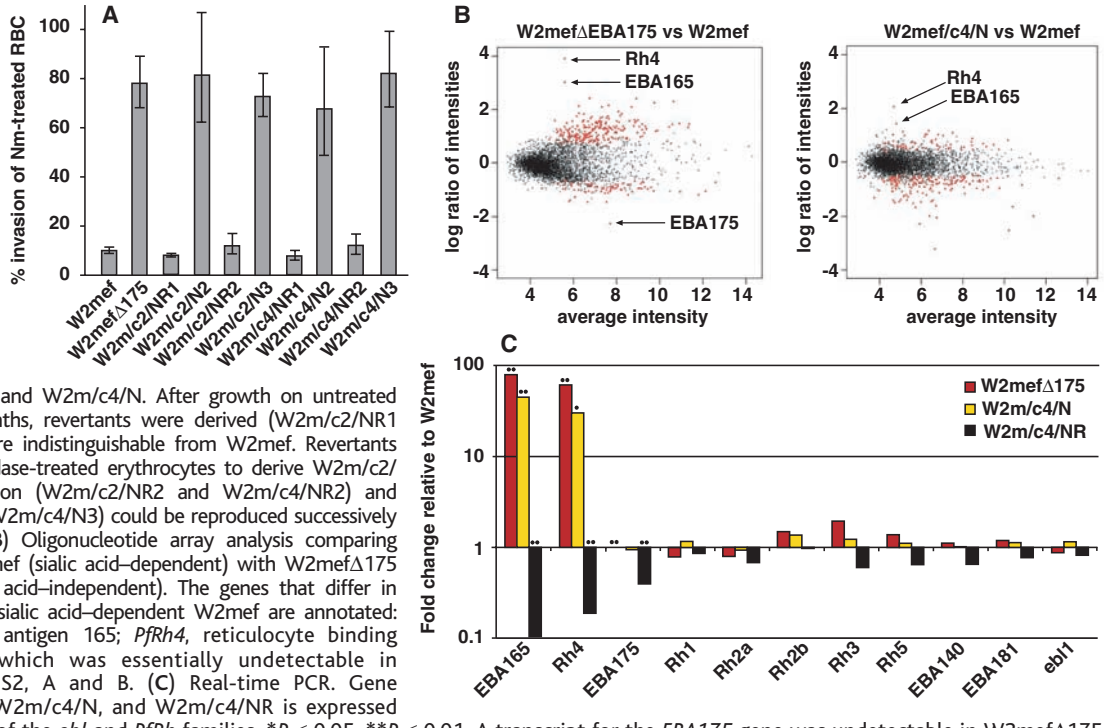

Fig. 1. Sialic acid–dependent and –independent invasion and global transcription in *P. falciparum*. (**A**) Erythrocytes were treated with neuraminidase to remove surface sialic acid residues. The percentage invasion into neuraminidase (Nm)–treated erythrocytes is shown relative to invasion into untreated erythrocytes. W2mefΔ175 has the *EBA175* gene disrupted (*6*). W2mef/c2 and c4 were cloned (fig. S1A) and selected for growth on neuraminidase-treated erythrocytes to obtain W2m/c2/N and W2m/c4/N. After growth on untreated erythrocytes over several months, revertants were derived (W2m/c2/NR1 and W2m/c4/NR1), which were indistinguishable from W2mef. Revertants were reselected on neuraminidase-treated erythrocytes to derive W2m/c2/N2 and W2m/c4/N2. Reversion (W2m/c2/NR2 and W2m/c4/NR2) and reselection (W2m/c2/N3 and W2m/c4/N3) could be reproduced successively in both clones of W2mef. (**B**) Oligonucleotide array analysis comparing transcriptional profiles in W2mef (sialic acid–dependent) with W2mefΔ175 and W2mef/c4/N (both sialic acid–independent). The genes that differ in transcription most relative to sialic acid–dependent W2mef are annotated: *EBA165*, erythrocyte binding antigen 165; *PfRh4*, reticulocyte binding homolog 4; and *EBA175*, which was essentially undetectable in W2mefΔ175. See also fig. S2, A and B. (**C**) Real-time PCR. Gene expression in W2mefΔ175, W2m/c4/N, and W2m/c4/NR is expressed relative to W2mef for genes of the *ebl* and *PfRh* families. $*P < 0.05$, $**P < 0.01$. A transcript for the *EBA175* gene was undetectable in W2mefΔ175. See also fig. S2C.

To address this issue, two clonal lines of W2mef, W2m/c2 and W2m/c4 (fig. S1A), were selected on neuraminidase-treated erythrocytes to select parasites switched to sialic acid–independent invasion to derive W2m/c2/N and W2m/c4/N, both of which showed invasion comparable to that of W2mefΔ175. These parasites were grown on normal erythrocytes for several months to derive W2m/c2/NR1 and W2m/c4/NR1, which had reverted to sialic acid–dependent invasion (Fig. 1A). Both revertant clones were reselected on neuraminidase-treated erythrocytes and invaded using sialic acid–independent receptors. Further rounds of growth on normal erythrocytes and reselection on neuraminidase-treated erythrocytes showed that the ability to switch invasion pathways was reproducible (Fig. 1A). The ability of W2mef to switch from sialic acid–dependent to –independent invasion is reversible and demonstrates the plasticity of *P. falciparum* in the face of selective pressures such as altered erythrocyte receptors.

Microarrays of *P. falciparum* (*7*) were used to reveal any transcriptional switch between W2mef versus W2mefΔ175 and W2m/c4/N (Fig. 1B and fig. S2, A and B). *PfRh4* (PFD1150c) (*8*) and *EBA165* (PFD1155w) were the only genes to show reproducible and significant transcriptional differences. *PfRh4* and *EBA165* occur within the *P. falciparum* genome in a head-to-head orientation on chromosome 4, and it is possible they are coregulated (*9*). The protein encoded by *PfRh4* is homologous to other reticulocyte binding–like

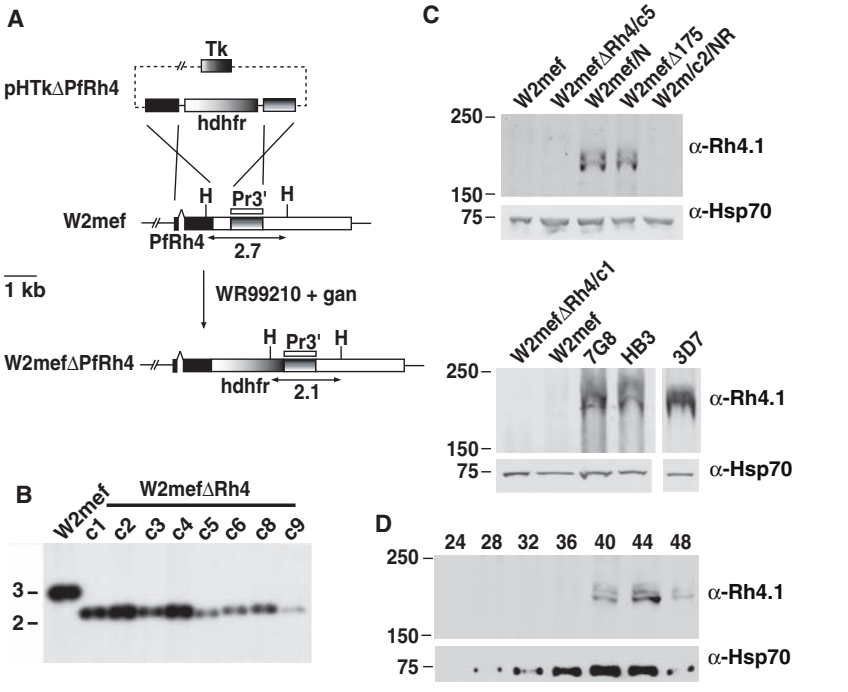

Fig. 2. Disruption of *PfRh4* and expression of PfRh4 protein in *P. falciparum*. (**A**) Schematic of the wild-type and disrupted *PfRh4* loci. The *hDHFR* gene was inserted into *PfRh4* by double crossover recombination. Southern analysis was performed using Hind III (H)–digested DNA with probe Pr3′. (**B**) Southern blot of the *PfRh4* locus in W2mef and clones of W2mefΔRh4 (fig. S1B). Clones 1 to 4 and clones 5 to 9 were derived from two independent transfections. Molecular sizes are shown on the left (in kb). The absence of the 2.7-kb wild-type band and the presence of a 2.1-kb band indicate that the *PfRh4* locus is disrupted in all clones. (**C**) Schizonts were probed with α-Rh4.1 (fig. S3B) (top) or α-Hsp70 (bottom) antibodies. W2mefΔ175 and W2mef/N (sialic acid–independent) express PfRh4, which was absent in W2mef, W2mefΔRh4/c5, W2mefΔRh4/c1, and W2m/c2/NR (sialic acid–dependent) parasites. Molecular sizes are indicated on the left (in kD). The parasite lines 7G8, HB3, and 3D7 also express PfRh4 and invade by sialic acid–independent pathways. (**D**) Expression of PfRh4 over the asexual life cycle is shown for W2mefΔ175, and time points are indicated in hours.

proteins (PfRh), including PfRh1 (PFD0110w) and PfRh2b (MAL13P1.176) that have been implicated in *P. falciparum* invasion of erythrocytes (*10*–*12*), and this family is related to other invasion proteins in *Plasmodium yoelii* (*13*) and *Plasmodium vivax* (*14*). *EBA165* is a member of the erythrocyte binding–like (ebl) family that includes EBA175; however, current data suggest that it is a transcribed pseudogene (*15*). Sequencing of *EBA165* in W2mefΔ175 and W2mef showed that frameshift mutations were present, suggesting that it was unlikely to encode a protein and was only activated by its proximity to *PfRh4*. Additionally, antibodies to putative EBA165 did not bind to the predicted protein in W2mefΔ175 (fig. S3A).

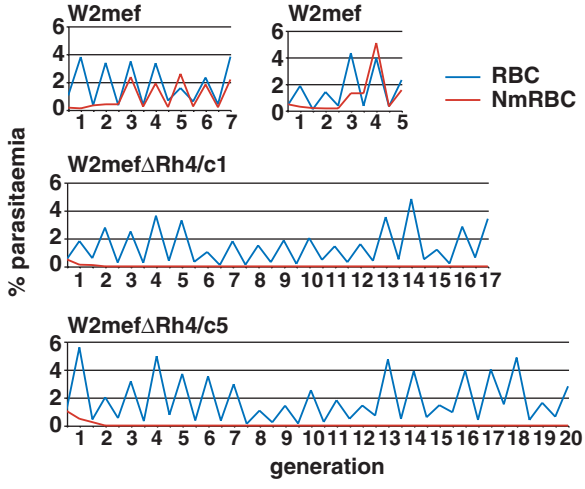

Fig. 3. Disruption of *PfRh4* blocks switching from sialic acid–dependent to –independent invasion of host erythrocytes. Parasites were grown on either untreated or neuraminidase-treated erythrocytes. Starting parasitemia was ~0.5%, and parasites were subcultured every 48 hours to prevent overgrowth. In two independent experiments, W2mef switched invasion pathway from sialic acid dependence to independence by generation 3 (day 6). W2mefΔRh4/c.1 and c.5 (derived from independent transfection experiments) were unable to switch to sialic acid–independent invasion, and no parasites were observed after extended culture on neuraminidase-treated red cells (up to 40 days) or after the culture had been returned to untreated erythrocytes. The same result was observed for all W2mefΔRh4 clones (fig. S3C).

To validate transcriptional changes seen in microarrays, we used real-time polymerase chain reaction (RT-PCR) of sialic acid–dependent parasites W2mef and W2m/c4/NR, and sialic acid–independent parasites W2mefΔ175 and W2m/c4/N (Fig. 1C and fig. S2C). Transcription of *PfRh4* and *EBA165* increased ~60- to 80-fold in the sialic acid–independent lines compared with the sialic acid–dependent lines, confirming the microarray results. In comparison, other members of the *ebl* and *PfRh* families showed relatively minor increases in transcription. These results suggest that activation of the *PfRh4* gene is required for switching from sialic acid–dependent to –independent invasion.

We constructed transgenic parasites in which the *PfRh4* gene was disrupted (W2mefΔRh4/c1-9) and used PfRh4-specific antibodies to determine expression patterns (Fig. 2 and fig. S3B). Attempts to disrupt *PfRh4* in the sialic acid–independent parasite lines 3D7 and 7G8 were unsuccessful; although this does not verify that *PfRh4* is essential in these sialic acid–independent parasites, it does suggest a functionally important role in the invasion of normal erythrocytes. Specific antibodies did not detect PfRh4 in sialic acid–dependent parasites W2mef and W2m/c4/NR, nor in any

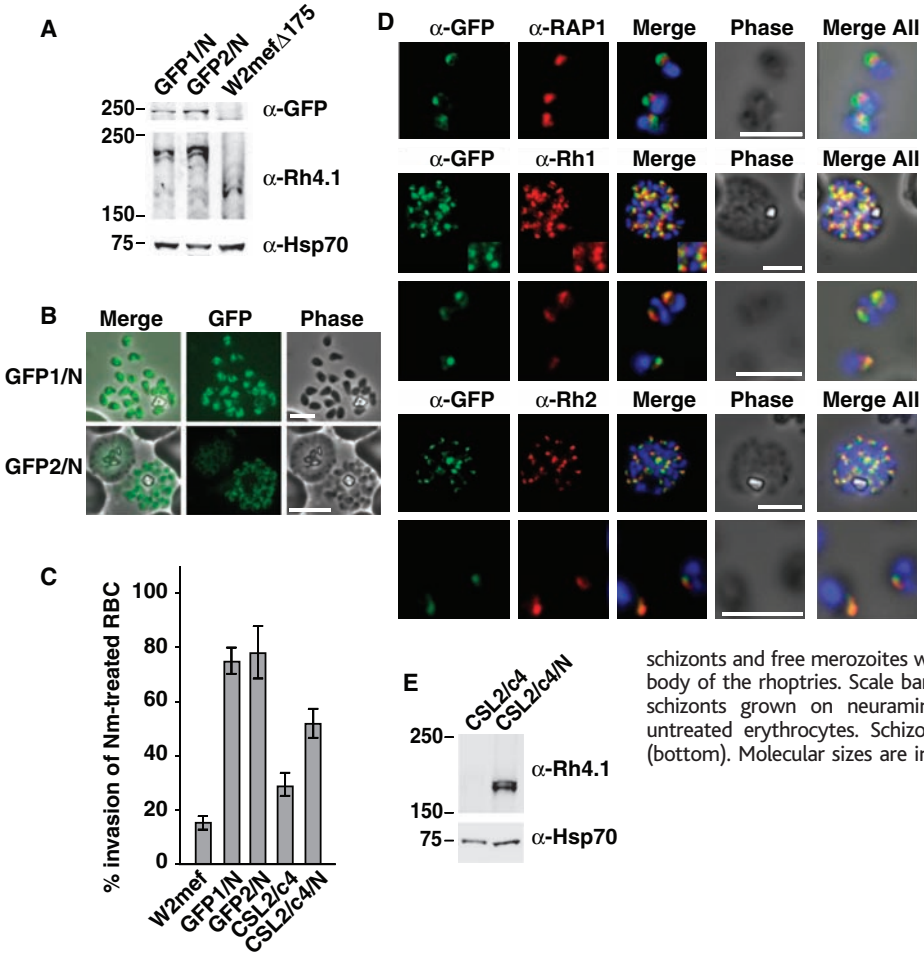

Fig. 4. Subcellular localization of PfRh4 in *P. falciparum* lines with different invasion pathways. (**A**) Two independent clones (fig. S1C), in which PfRh4 is tagged with GFP (see fig. S5, A to C for construction details), were selected for sialic acid–independent invasion by growth on neuraminidase (Nm)–treated erythrocytes. Western analysis of sialic acid–independent W2mef-Rh4GFP/N clones [W2mef-Rh4GFP1/N (GFP1/N) and W2mef-Rh4GFP2/N (GFP2/N)] shows that the PfRh4-GFP chimeric protein was larger than the endogenous form and no GFP-tagged protein was detected in W2mefΔ175. Molecular sizes are indicated on the left (in kD). (**B**) GFP1/N and GFP2/N showed fluorescence, and in many cases it was possible to localize the GFP to the apical tip of merozoites (see also fig. S5D). (**C**) Invasion of W2mef, GFP1/N, GFP2/N, CSL2/c4 and CSL2/c4/N into neuraminidase-treated erythrocytes. The *P. falciparum* strain CSL2 was cloned (fig. S1D) and grown on neuraminidase-treated erythrocytes. (**D**) PfRh4 colocalizes with PfRh1 and PfRh2 in schizonts (also see enlargements, second row of panels) and merozoites. W2mef-Rh4GFP1/N was used to test colocalization with PfRh1, PfRh2, and RAP1. All proteins localize to the apical pole and show pronounced overlap in segmenting schizonts and free merozoites with the exception of RAP-1, which is localized to the body of the rhoptries. Scale bar, 5 μm. (**E**) PfRh4 is expressed more highly in CSL2 schizonts grown on neuraminidase-treated erythrocytes (CSL2/c4/N) than on untreated erythrocytes. Schizonts were probed with α-Rh4.1 (top) or α-Hsp70 (bottom). Molecular sizes are indicated on the left (in kD).

of the W2mefΔRh4 cloned lines (Fig. 2C). In contrast, PfRh4 was expressed in sialic acid–independent lines W2mef/N and W2mefΔ175, as well as in 7G8, HB3, and 3D7. Western analysis was performed during the course of the 48-hour asexual blood stage life cycle of W2mefΔ175 parasites. PfRh4 was detected in mature schizonts (Fig. 2D), concomitant with apical organelle development and expression of other ligands involved in the invasion process (*1*, *16*).

W2mΔRh4 parasites were grown on normal or neuraminidase-treated erythrocytes to determine if they could switch to sialic acid–independent invasion. W2mefΔEBA181 parasites (*17*) were generated in the same way as W2mefΔRh4, and as expected, this line was able to switch to sialic acid–independent invasion (fig. S4A). Although W2mΔRh4 parasites grew normally on untreated erythrocytes (Fig. 3), they were unable to switch to sialic acid–independent invasion even after extended culture on neuraminidase-treated erythrocytes (Fig. 3 and fig. S3C), suggesting that invasion was completely blocked at the first generation. Therefore, transcriptional activation of the *PfRh4* gene and expression of the PfRh4 protein are required for switching of W2mef from sialic acid–dependent to –independent invasion.

We constructed two independent transgenic parasite lines that expressed PfRh4 as a chimeric protein with green fluorescent protein (GFP) to determine if subcellular localization of PfRh4 is consistent with a role in merozoite invasion; the results were identical (figs. S1C and S5). The W2mef-Rh4GFP parasites could switch invasion pathways and invaded neuraminidase-treated erythrocytes efficiently, indicating that activation and function of PfRh4 were preserved (Fig. 4C). The GFP-tagged PfRh4 protein showed the expected increase in molecular weight (Fig. 4A). Segmenting schizonts and merozoites of W2mef-Rh4GFP1N/2N displayed fluorescence apical to the nucleus (Fig. 4B, fig. S5D). PfRh4 colocalized well with PfRh2a/b in segmenting schizonts, and the overlap condensed into a single apical dot in free merozoites in which PfRh2a and b are present in the neck of the rhoptries (*11*, *12*) (Fig. 4D). PfRh4 was more apical than RAP1, a protein located within the body of the rhoptries (*18*). Therefore, PfRh4 is located at the apical tip of free merozoites, consistent with a direct function in invasion of erythrocytes.

We tested several sialic acid–dependent strains for growth on neuraminidase-treated erythrocytes to determine if the ability to switch invasion pathways and use different receptors for invasion is a general property of *P. falciparum*. Cloned lines of CSL2 (fig. S1D) were sialic acid–dependent but adapted to sialic acid–independent invasion in a similar way to W2mef (Fig. 4C) in association with elevated expression of PfRh4 protein (Fig. 4E).

We have shown that activation of sialic acid–independent invasion is regulated by differential gene expression and silencing of *PfRh4*. Activation of *PfRh4* occurs at a low level, and these variant parasites can be selected by growth on erythrocytes lacking sialic acid or by genetic ablation of the *EBA175* gene. Silencing of the active *PfRh4* gene occurs over time when parasites are returned to normal erythrocytes, showing that the switch in invasion pathways can occur in both directions in the presence of functional EBA175. The activation of *PfRh4* in response to loss of EBA175 function suggests that the PfRh and ebl protein families show some overlap with respect to their function in invasion. The ability to switch receptor usage for invasion from sialic acid–dependent to –independent pathways represents a previously unknown strategy to evade host receptor polymorphisms and immune mechanisms and has important implications for the design of vaccines against malaria parasites.

References and Notes

1. J. W. Barnwell, M. R. Galinski, in *Malaria: Parasite Biology, Pathogenesis and Protection*, I. W. Sherman, Ed. (American Society for Microbiology, Washington, DC, 1998), pp. 93–120.
2. V. C. Okoye, V. Bennett, *Science* **227**, 169 (1985).
3. J. Baum, M. Pinder, D. J. Conway, *Infect. Immun.* **71**, 1856 (2003).
4. S. A. Dolan, L. H. Miller, T. E. Wellems, *J. Clin. Invest.* **86**, 618 (1990).
5. M. B. Reed *et al.*, *Proc. Natl. Acad. Sci. U.S.A.* **97**, 7509 (2000).
6. M. T. Duraisingh, A. G. Maier, T. Triglia, A. F. Cowman, *Proc. Natl. Acad. Sci. U.S.A.* **100**, 4796 (2003).
7. K. G. Le Roch *et al.*, *Science* **301**, 1503 (2003).
8. O. Kaneko, J. Mu, T. Tsuboi, X. Su, M. Torii, *Mol. Biochem. Parasitol.* **121**, 275 (2002).
9. M. J. Gardner *et al.*, *Nature* **419**, 498 (2002).
10. J. C. Rayner, M. R. Galinski, P. Ingravallo, J. W. Barnwell, *Proc. Natl. Acad. Sci. U.S.A.* **97**, 9648 (2000).
11. J. C. Rayner, E. Vargas-Serrato, C. S. Huber, M. R. Galinski, J. W. Barnwell, *J. Exp. Med.* **194**, 1571 (2001).
12. M. T. Duraisingh *et al.*, *EMBO J.* **22**, 1047 (2003).
13. P. R. Preiser, W. Jarra, T. Capiod, G. Snounou, *Nature* **398**, 618 (1999).
14. M. R. Galinski, C. C. Medina, P. Ingravallo, J. W. Barnwell, *Cell* **69**, 1213 (1992).
15. T. Triglia, J. K. Thompson, A. F. Cowman, *Mol. Biochem. Parasitol.* **116**, 55 (2001).
16. A. F. Cowman *et al.*, *FEBS Lett.* **476**, 84 (2000).
17. T. W. Gilberger *et al.*, *J. Biol. Chem.* **278**, 14480 (2003).
18. G. R. Bushell, L. T. Ingram, C. A. Fardoulys, J. A. Cooper, *Mol. Biochem. Parasitol.* **28**, 105 (1988).

19. We thank T. Pappenfuss and M. Ritchie for help with statistical analysis, R. Good for technical assistance, and the Red Cross Blood Service for supply of human erythrocytes and serum. J.S. is supported by a Melbourne Research Scholarship and by the Australian Government's Cooperative Research Centre's Program. A.F.C. is supported by an International Research Scholarship from the Howard Hughes Medical Institute. This work is supported by the National Health and Medical Research Council of Australia and the Wellcome Trust. The microarray data have been deposited with The Gene Expression Omnibus (www.ncbi.nih.gov/projects/geo/) (Experiment ID: GSE2878).

Supporting Online Material

www.sciencemag.org/cgi/content/full/309/5739/1384/DC1
Materials and Methods
SOM Text
Figs. S1 to S5
References

24 May 2005; accepted 5 July 2005
10.1126/science.1115257

Computational Improvements Reveal Great Bacterial Diversity and High Metal Toxicity in Soil

Jason Gans, Murray Wolinsky, John Dunbar

The complexity of soil bacterial communities has thus far confounded effective measurement. However, with improved analytical methods, we show that the abundance distribution and total diversity can be deciphered. Reanalysis of reassociation kinetics for bacterial community DNA from pristine and metal-polluted soils showed that a power law best described the abundance distributions. More than one million distinct genomes occurred in the pristine soil, exceeding previous estimates by two orders of magnitude. Metal pollution reduced diversity more than 99.9%, revealing the highly toxic effect of metal contamination, especially for rare taxa.

For any complex system, the number and relative abundance of parts is fundamental to a quantitative description of the system. Quantification provides a framework to compare equilibrium and dynamic properties and, for biological communities, to evaluate perturbations such as pollution, global climate change, and foreign species encroachment. To quantify plant and animal communities, ecologists survey the number and relative abundance of species (i.e., species-abundance distributions) (*1*, *2*). However, effective measurement of bacterial species-abundance distributions has eluded

Bioscience Division, Los Alamos National Laboratory, Los Alamos, NM 87501, USA.